

Full photon statistics of a light beam transmitted through an optomechanical system

Andreas Kronwald,^{1,*} Max Ludwig,¹ and Florian Marquardt^{1,2}

¹*Friedrich-Alexander-Universität Erlangen-Nürnberg, Staudtstr. 7, D-91058 Erlangen, Germany*

²*Max Planck Institute for the Science of Light, Günther-Scharowsky-Straße 1/Bau 24, D-91058 Erlangen, Germany*

In this paper, we study the full statistics of photons transmitted through an optical cavity coupled to nanomechanical motion. We analyze the entire temporal evolution of the photon correlations, the Fano factor, higher moments of the photon distribution, and the effects of strong laser driving. In the regime of single-photon strong coupling, this allows us to predict interesting effects such as a transition from antibunching to bunching for larger observation time intervals and photon avalanches triggered by multi-photon absorption.

PACS numbers: 42.50.Ar, 42.50.Lc, 07.10.Cm, 42.65.-k

Introduction – The field of cavity optomechanics, where an optical mode couples to nanomechanical vibrations, has seen tremendous progress during the past few years. It is driven by the goals of probing the quantum motion of nanomechanical devices, implementing ultrasensitive measurements, and exploiting the light-mechanics coupling for quantum information processing (for reviews see e.g. [1, 2]). Recently, the mechanical degree of freedom was cooled down close to its quantum ground state using optomechanical sideband cooling [3, 4]. Thus, it now becomes important to analyze probes for the quantum dynamics of these systems. Experimentally, the most straightforward access is provided by the light field. In this context, the photon statistics represents a particularly powerful tool, as it is very sensitive to interactions and reveals the temporal correlations produced by the dynamics. A first study in this direction recently led to the prediction of photon blockade [5] in optomechanical systems. Here, we will take a significant step further by analyzing the full statistics of the stream of transmitted photons. In contrast to the earlier work, this allows us to study many new aspects, including strong laser driving, the full temporal structure of photon correlations, the Fano factor, and higher moments of the distribution of transmitted photons. All of these properties become particularly interesting in the regime of single-photon strong light-mechanics coupling, which (although challenging) is now being approached experimentally [3, 4, 6–8]. In this regime, the single photon coupling rate becomes comparable to the photon decay rate, and a few remarkable phenomena have already been predicted. A “classical to quantum crossover” may be observed in nonlinear optomechanical dynamics [9], photon blockade [5], non-Gaussian [10] and nonclassical [11] mechanical states might be produced, diverse Schrödinger-cat states could be generated [12, 13], and QND photon and phonon readout and nonlinearities could be enhanced in appropriate two mode setups [14, 15].

In this paper, we will first consider the photon statistics under weak laser drive, to make contact to previous works. Using quantum jump trajectory simulations, we will obtain the photon correlations at all time scales,

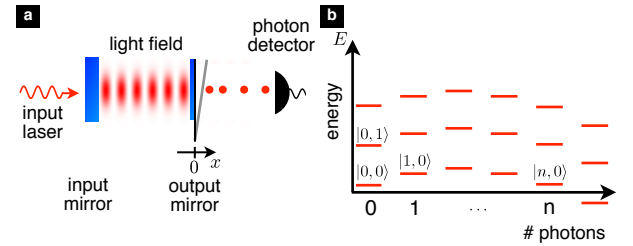


Figure 1: (a) The standard optomechanical setup, where photons are transmitted and detected by a photon detector. (b) Nonlinear level scheme induced by the light-mechanics coupling. The corresponding eigenstates read $|n_a, n_b\rangle$, where n_a denotes the number of photons and n_b the number of phonons.

discuss the Fano factor obtained from photon counting, and point out that there are regimes where the bunching/antibunching character depends on the time scale considered. Then we will turn to strong driving, where multi-photon transitions can become possible. We identify a special regime of “photon avalanches”, where photon absorption triggers a cascade of photon transmission through the optomechanical system. There, the light-mechanics interplay is particularly important in affecting the dynamics.

The Model – We consider the standard optomechanical setup consisting of a laser-driven optical cavity, see Fig. 1a. One of the end-mirrors is attached to a vibrating resonator, such that the cavity resonance frequency $\omega_{\text{cav}}(\hat{x})$ depends on the mirror-position \hat{x} . The coherent dynamics of this setup is described by the standard [1, 2] Hamiltonian

$$\hat{H} = -\hbar\Delta\hat{a}^\dagger\hat{a} - \hbar g_0 (\hat{b}^\dagger + \hat{b}) \hat{a}^\dagger\hat{a} + \hbar\Omega\hat{b}^\dagger\hat{b} + \hbar\alpha_L (\hat{a}^\dagger + \hat{a}), \quad (1)$$

written in the frame rotating at the laser frequency ω_L . Here, \hat{a} (\hat{b}) is the photon (phonon) annihilation operator, $\Delta = \omega_L - \omega_{\text{cav}}(0)$ is the laser detuning from resonance, and $g_0 = x_{\text{ZPF}} \cdot (\partial_x \omega_{\text{cav}}(x))|_{x=0}$ is the single-photon optomechanical coupling constant. Ω , m , and $x_{\text{ZPF}} = \sqrt{\hbar/2m\Omega}$ are the frequency, mass, and the zero-

point fluctuations of the resonator, respectively, whereas α_L is the laser driving amplitude. The full dissipative dynamics of the open optomechanical system can be described by a Lindblad master equation

$$\dot{\hat{\rho}} = \frac{i}{\hbar} [\hat{\rho}, \hat{H}] + \kappa_I \mathcal{D}[\hat{a}]\hat{\rho} + \Gamma_M \mathcal{D}[\hat{b}]\hat{\rho} - \frac{\kappa_O}{2} \{\hat{a}^\dagger \hat{a}, \hat{\rho}\} + \kappa_O \hat{a} \hat{\rho} \hat{a}^\dagger, \quad (2)$$

where $\hat{\rho}$ is the density matrix for the photons and phonons. κ_I (κ_O) is the photon loss rate through the input (output) mirror, whereas Γ_M is the phonon decay rate. The standard Lindblad dissipation superoperator reads $\mathcal{D}[\hat{a}]\hat{\rho} = \hat{a}\hat{\rho}\hat{a}^\dagger - \{\hat{a}^\dagger \hat{a}, \hat{\rho}/2\}$, where $\{\hat{a}, \hat{c}\} = \hat{a}\hat{c} + \hat{c}\hat{a}$ is the anticommutator.

Photons and phonons can be decoupled by applying the polaron transformation [12, 13] $\hat{H}' = \hat{U}^\dagger \hat{H} \hat{U}$ to Eq. (1), where $\hat{U} = \exp[g_0 \hat{a}^\dagger \hat{a} (\hat{b}^\dagger - \hat{b})/\Omega]$. This yields

$$\begin{aligned} \hat{H}' = & -\hbar \Delta \hat{a}^\dagger \hat{a} + \hbar \Omega \hat{b}^\dagger \hat{b} - \hbar \frac{g_0^2}{\Omega} (\hat{a}^\dagger \hat{a})^2 \\ & + \hbar \alpha_L (\hat{a}^\dagger \hat{D}^\dagger + \text{H.c.}), \end{aligned} \quad (3)$$

where the mechanical displacement operator $\hat{D} = \exp[g_0(\hat{b}^\dagger - \hat{b})/\Omega]$ now enters the transformed driving term. Note that the elimination of the photon-phonon coupling has given rise to a photon interaction term. This will lead to an anharmonic photon energy level scheme, cf. Fig. 1b, which drastically influences the intracavity photon statistics if $g_0^2 \gtrsim \kappa \Omega$ [5].

Quantum Jump Trajectory Method – In an experiment, one is able to analyze the photon statistics by measuring the times t_n when a photon leaves the cavity through the output mirror. To simulate this detection process, we will use the quantum jump trajectory method [16–20], which can be understood as an “unraveling” of the master equation. It has recently been employed to discuss single-phonon detection in optomechanical systems [21].

If a photon was detected (a “photon jump” occurred) during a time interval $[t, t + \delta t]$, then the information about the system is updated according to

$$\hat{\rho}(t + \delta t) = \frac{\hat{a} \hat{\rho}(t) \hat{a}^\dagger}{\text{Tr}(\hat{a}^\dagger \hat{a} \hat{\rho}(t))}. \quad (4)$$

The probability of this event is given by $p_j = \kappa_O \langle \hat{a}^\dagger \hat{a} \rangle(t) \delta t$ (Note that we assume unit detection efficiency). This corresponds to the unraveling of the second line of Eq. (2).

If no photon leaves the output port, then the state $\hat{\rho}$ evolves according to the first line of Eq. (2), but it will have to be renormalized after each time step. This evolution describes the increase of our knowledge due to the absence of a detection event [18, 22]. Overall, we obtain stochastic traces of photon detection events which directly correspond to what would be observed

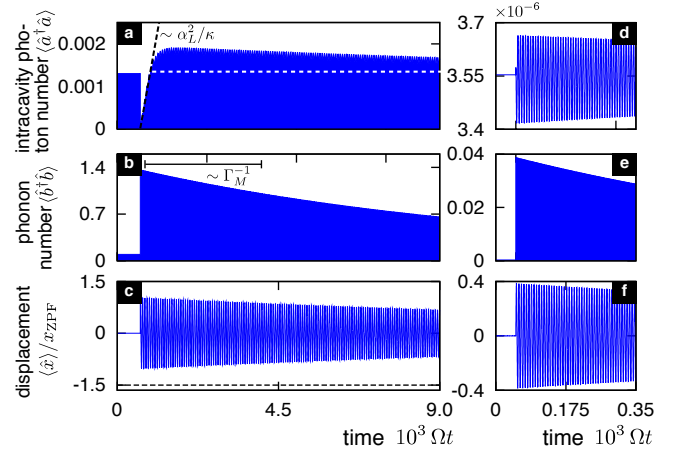


Figure 2: Typical quantum jump trajectories for a weakly driven optomechanical system. These show the expectations for the photon number (a,d), phonon number (b,e), and displacement (c,f), evolving conditioned on the detection of a photon leaving the cavity at a certain time. The concomitant sudden drop in the radiation pressure force leads to subsequent mechanical oscillations, relaxing during the damping time Γ_M^{-1} . (a-c) Sideband-resolved regime ($\kappa = \Omega/8$), with $g_0/\kappa = 4$. (b-f) Bad cavity limit ($\kappa = 5\Omega$, and $g_0/\kappa = 1/10$). [Parameters: blue detuning $\Delta = \Omega - g_0^2/\Omega$, coupling $g_0 = \Omega/2$, laser drive $\alpha_L = 5 \cdot 10^{-3} \Omega$, mechanical damping $\Gamma_M = 10^{-3} \Omega$, photon decay $\kappa_I = \kappa_O = \kappa/2$. Size of Hilbert space: $n_a^{\max} = 4$, $n_b^{\max} = 9$]

in an experiment. Thereby, we gain access to the full statistics, including arbitrary moments and the complete time-dependence of photon correlations.

Full Counting Statistics – The full counting statistics $p(N, T_S)$ [23] is given by the probability of measuring N photons leaving the cavity in a sampling time interval T_S , for a constant rate $\dot{N} = \kappa_O \bar{n}$ of transmitted photons. Here, \bar{n} is the steady state photon number of the (full) master equation (2). The fluctuations of the detected photon number can be characterized via the counting Fano factor

$$\mathcal{F}_{\text{count}}(T_S) = \left(\langle N^2 \rangle - \langle N \rangle^2 \right) / \langle N \rangle, \quad (5)$$

where $\langle N^m \rangle = \sum_{N=0}^{\infty} N^m p(N, T_S)$. If $\mathcal{F}_{\text{count}}(T_S) < 1$ there is antibunching (on that observation time-scale), whereas for $\mathcal{F}_{\text{count}}(T_S) > 1$ the photons are bunched. Note that the counting Fano factor \mathcal{F} is connected to the two-photon correlation function $g^{(2)}(\tau) = \langle \hat{a}^\dagger(0) \hat{a}^\dagger(\tau) \hat{a}(\tau) \hat{a}(0) \rangle / \bar{n}^2$ via [23]

$$\mathcal{F}_{\text{count}}(T_S) = 1 + \dot{N} \int_{-T_S}^{T_S} d\tau \left(g^{(2)}(|\tau|) - 1 \right) (1 - |\tau|/T_S). \quad (6)$$

The long-time limit of the Fano factor then directly yields the zero-frequency shot noise power, $S(\omega = 0) = \lim_{T_S \rightarrow \infty} (\text{Var } N)/T_S = \dot{N} \mathcal{F}_{\text{count}}(T_S \rightarrow \infty)$.

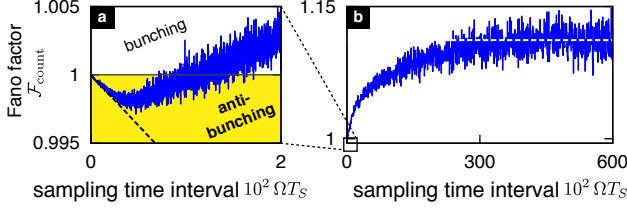


Figure 3: Fano factor $\mathcal{F}_{\text{count}}(T_S)$ for photon detection events, as a function of the sampling time interval T_S . (a) Fano factor for small sampling times, where antibunching is observed ($g^{(2)}(0) < 1$ and $\mathcal{F}(T_S) < 1$; cf. Eq. (6)). The black dashed line is a plot of the short-time solution of Eq. (6), where $\langle \hat{a}^\dagger \hat{a} \rangle$ and $g^{(2)}(0)$ are extracted from a steady-state solution of the master equation (2). (b) Fano factor for larger sampling times T_S . We see that $\mathcal{F}_{\text{count}}(T_S \rightarrow \infty) > 1$ saturates and indicates photon bunching. This is a crucial effect of the mechanical motion induced by a photon jump (see main text). [Parameters as in Fig. 2a. Total simulation time $\Omega T_{\text{sim}} = 2 \cdot 10^8$, number of jumps $\sim 10^4 \sim \dot{N} T_{\text{sim}}$].

In the following, we will use the Fano factor to analyze the photon statistics of an optomechanical system in the interesting regime of single-photon strong coupling $g_0 \sim \kappa$ (and $g_0 \sim \Omega$).

Weak Laser Drive – Here, we start by considering a weak drive such that the photon number inside the cavity remains small, $\langle \hat{a}^\dagger \hat{a} \rangle \ll 1$. This is useful to connect to previous results [5], in contrast to which we will be able to discuss the photon correlations $g^{(2)}(\tau)$ at arbitrary time-delays.

Fig. 2a-c shows a typical trajectory in the photon-blockade regime [5], where the intracavity photon number $\langle \hat{a}^\dagger \hat{a} \rangle$ inside the cavity decreases due to a photon jump [22] (it would stay constant for a coherent state). In general, this single detected photon must have exerted a radiation force up to the time it leaves the cavity. Thus, upon detection the expectation for the mechanical displacement is updated to reflect the value it must have had due to this force (sudden jump of $\langle \hat{x} \rangle$ in Fig. 2c towards a greater displacement). The subsequent oscillation decays on the mechanical damping time scale. These effects could be observed by pulsed displacement measurements conditioned on photon detection events. The photon number itself quickly increases again due to the laser driving and then, more slowly on a scale Γ_M^{-1} , settles to its limiting value.

In the following, we will focus on the effects of this backaction onto the two-photon correlations for time delays $\tau \neq 0$. As can be seen in Fig. 2a, where blue detuning is chosen, the photon number temporarily exceeds its limiting value before settling down. This is because the mechanical oscillations bring the cavity closer to resonance. Thus, even though at very short times photon antibunching is clearly present, longer observation times will feature photon bunching for blue detuning $\Delta > 0$. It

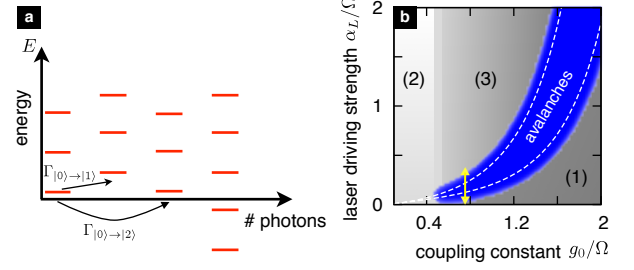


Figure 4: (a) Optomechanical level scheme for a choice of red detuning that enables two-photon transitions. (b) Map of parameters α_L and g_0/Ω , for which avalanche-like behavior is expected (dark blue region). Note that in regions (1), (2) and (3) the first, second and third inequality of Eq. (9) is violated. The arrow indicates the trace taken in Fig. 5. [Parameters: $\Delta = -2g_0^2/\Omega$ and $g_0/\kappa = 4$]

should be noted that this is a crucial effect of the mechanical motion and would not be discovered in any analysis of the short-time correlations $g^{(2)}(\tau = 0)$.

Let us now quantify this by considering the Fano factor $\mathcal{F}_{\text{count}}(T_S)$ as a function of the sampling time interval T_S , as shown in Fig. 3. For the bad cavity case displayed in Fig. 2d-f, the Fano factor would be close to the value expected for a simple coherent laser beam, $\mathcal{F}_{\text{count}}(\infty) \approx 1$. In contrast, for the strongly coupled optomechanical system of Fig. 2a-c, it shows pronounced antibunching at short times ($\mathcal{F} < 1$) and bunching ($\mathcal{F} > 1$) for long times, up to $T_S \rightarrow \infty$.

In conclusion, we emphasize that $\mathcal{F}_{\text{count}}(T_S)$ has to be analyzed for all sampling times T_S to capture the full impact of the optomechanical dynamics on the photon statistics. Even the sign of the effect (bunching vs. antibunching) can depend on the observation time interval.

Photon Avalanches at Strong Driving – At strong driving, multi-photon transitions can take place. There, n photons enter the cavity simultaneously, since other possibilities are precluded by energy conservation due to the optomechanically induced photon nonlinearity. We will see that if the parameters are suitable, this can give rise to “avalanches” of much more than n photons being transmitted.

Such a situation can be evoked by choosing red detuning, $\Delta = -n \cdot g_0^2/\Omega$. Then, multi-photon absorption of $n > 1$ photons becomes possible and involves $n - 1$ virtual transition steps. To favor this virtual (but resonant) $|0\rangle \rightarrow |n\rangle$ transition over the non-virtual (but off-resonant) absorption of one photon ($|0\rangle \rightarrow |1\rangle$), we have to compare the corresponding transition rates (cf. Fig. 4a)

$$\Gamma_{|0\rangle \rightarrow |1\rangle} = \alpha_L^2 \frac{\kappa}{(n-1)^2 g_0^2/\Omega^2 + \kappa^2/4} \quad (7)$$

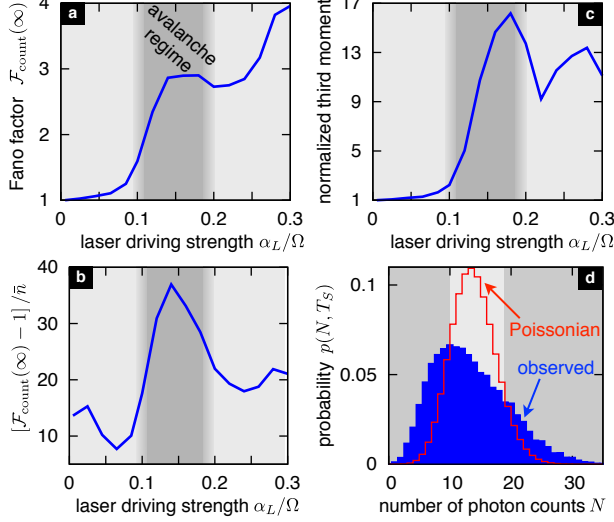


Figure 5: Photon statistics in the “photon avalanche regime”. (a) Fano factor $\mathcal{F}_{\text{count}}(\infty)$ in the long-time limit, as a function of laser drive. The highlighted region is the region where multi-photon absorption is favored (cf. Fig. 4b). At the onset of this regime, the Fano factor $\mathcal{F}_{\text{count}}$ suddenly rises. (b) Rescaled deviation from Poisson statistics. (c) Normalized third moment, $\langle (N - \langle N \rangle)^3 \rangle / \langle N \rangle$. (d) Distribution of photon counts showing strong deviation from a Poissonian distribution with same mean. [Parameters: $\Delta = -2g_0^2/\Omega$, $g_0 = \Omega/\sqrt{2}$, $\kappa = \Omega/(4\sqrt{2})$, $\Gamma_M = 10^{-3}\Omega$. Maximal size of Hilbert space: $n_a^{\text{max}} = 5$, $n_b^{\text{max}} = 36$. (d): $\alpha_L = 0.14\Omega$, $\Omega T_S = 3000$].

and

$$\Gamma_{|0\rangle \rightarrow |n\rangle} = \frac{4\alpha_L^{2n}}{\kappa} \left(\frac{\Omega}{g_0^2} \right)^{2(n-1)} \frac{1}{[(n-1)!]^3}. \quad (8)$$

We impose the inequalities

$$\Gamma_{|0\rangle \rightarrow |n\rangle} > \Gamma_{|0\rangle \rightarrow |1\rangle}, \quad \kappa \ll |\Delta_n|, \quad \text{and} \quad \kappa \gg \Gamma_{|0\rangle \rightarrow |n\rangle} \quad (9)$$

to favor the resonant transition, to ensure that the intermediate transitions of the resonant transition are virtual, and to prevent heating of the resonator. Upon increasing the laser drive, at some point n -photon absorption will start to be favored over other processes. Neglecting the mechanical motion, we expect that these n photons will decay out of the cavity on a timescale $\sim \kappa^{-1}$, leading to photon bunching. In this case, naive expectation holds that $\mathcal{F}_{\text{count}}(\infty) \approx n$. Thus, the Fano factor has to increase when multi-photon absorption starts to become important.

For the simulations, we will focus on the case $n = 2$, such that $n = 0$ and $n = 2$ are resonant, cf. Fig. 4a, but the following explanations should hold in general. Furthermore, we will focus on single-photon strong coupling $g_0 \gtrsim \kappa$. The remaining free parameters are the laser driving strength α_L and the ratio g_0/Ω . A map of these

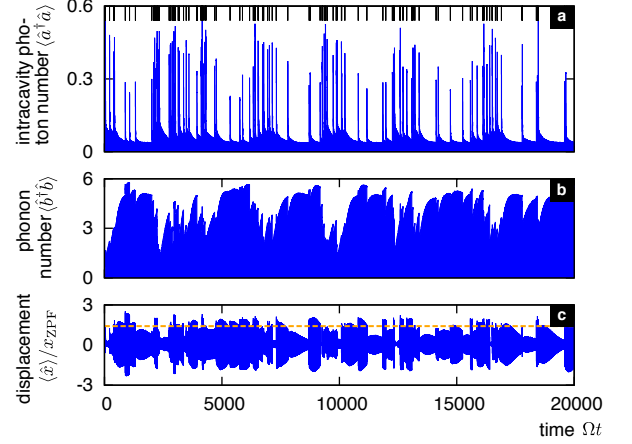


Figure 6: Typical quantum jump trajectory in a regime where avalanches are observable due to two-photon absorption. The pattern of vertical lines in (a) indicates the actual photon jump events, where bunching is clearly observable. The orange, dashed line in (c) corresponds to the displacement that would make the cavity resonant with the incoming laser. [Parameters: as in Fig. 5, and $\alpha_L = 0.15\Omega$. Size of Hilbert space: $n_a^{\text{max}} = 5$, $n_b^{\text{max}} = 15$].

two parameters is shown in Fig. 4b, where the regime fulfilling the inequalities (9) is highlighted.

In Fig. 5a, the Fano factor $\mathcal{F}_{\text{count}}(\infty)$ is shown as a function of the laser drive. We see that $\mathcal{F}_{\text{count}} \approx 1$ for weak laser driving (Poisson statistics), while $\mathcal{F}_{\text{count}}(\infty)$ increases rapidly beyond the threshold of the laser drive predicted by the above analysis. There, multi-photon absorption is favored and photons are emitted in bunches, cf. Fig. 5d. In contrast to our naive expectation, $\mathcal{F}_{\text{count}}(\infty)$ is larger than $n = 2$. This fact is due to the mechanical motion induced by the arrival of multiple photons inside the cavity:

In Fig. 6, we display a typical jump trajectory with multi-photon absorption events. Upon detection of a photon leaving the cavity, the expected intracavity photon number actually increases. This behavior is known for situations with photon bunching [22, 24], and it arises because the detection of a photon is most likely due to a previous multi-photon absorption. The remaining photons are likely to be emitted rapidly afterwards. However, the mechanical motion induced by the photon jump (originally discussed above in our analysis of the weak-coupling case) now can bring the cavity closer into resonance, which allows for the transmission of additional photons. In this way, avalanches of more than n photons become possible ($\mathcal{F}_{\text{count}}(\infty) > n$). Note that once a single avalanche process terminates, no photon jumps are observed any more and the mechanical displacement is able to relax towards its equilibrium value.

For even larger driving strengths, where the third in-

equality of Eq. (9) is violated, the average photon and phonon numbers as well as $\mathcal{F}_{\text{count}}(\infty)$ increase even further. Additionally, no clear avalanches are observable anymore. However, the strong photon noise in that case can be explained as being due to the transmission modulated stochastically by a fluctuating mirror, whose motion has been heated. This can be seen most clearly from an inspection of the rescaled Fano factor, $(\mathcal{F}_{\text{count}} - 1)/\bar{n}$ (Fig. 5b). Note that the statistical data obtained from the quantum jump trajectory simulations (involving $\sim 10^5$ photons) also provide access to higher moments and the full counting statistics at arbitrary observation time intervals. The third moment (Fig. 5c), for example, displays features such as a maximum in the “avalanche regime” studied here.

Conclusion – We have analyzed the full statistics of photons transmitted through an optomechanical system, based on quantum jump trajectory simulations. One finds that the photon correlations crucially depend on the observation time and may even change from antibunching to bunching in the long-time limit. For larger laser driving, photon avalanches may be observed, where the Fano factor strongly rises, beyond the values predicted in a naive analysis. These phenomena rely heavily on the light-mechanics coupling and the long relaxation times introduced by the mechanical system.

Acknowledgments – Financial support by DARPA ORCHID, the Emmy-Noether program and the ERC is gratefully acknowledged. A.K. thanks the HPC group at the FAU Erlangen-Nürnberg for stimulating discussions.

-
- [1] T. J. Kippenberg and K. J. Vahala, *Science* **321**, 1172 (2008).
 - [2] F. Marquardt and S. M. Girvin, *Physics* **2**, 40 (2009).
 - [3] J. D. Teufel *et al.*, *Nature* **475**, 359 (2011).
 - [4] J. Chan *et al.*, *Nature* **478**, 89 (2011).
 - [5] P. Rabl, *Phys. Rev. Lett.* **107**, 063601 (2011).
 - [6] K. W. Murch *et al.*, *Nat Phys* **4**, 561 (2008).
 - [7] F. Brennecke *et al.*, *Science* **322**, 235 (2008).
 - [8] E. Verhagen *et al.*, *Nature* **482**, 63 (2012).
 - [9] M. Ludwig, B. Kubala, and F. Marquardt, *New J. Phys.* **10**, 095013 (2008).
 - [10] A. Nunnenkamp, K. Børkje, and S. M. Girvin, *Phys. Rev. Lett.* **107**, 063602 (2011).
 - [11] J. Qian *et al.*, arXiv:1112.6200.
 - [12] S. Mancini, V. I. Man’ko, and P. Tombesi, *Phys. Rev. A* **55**, 3042 (1997).
 - [13] S. Bose, K. Jacobs, and P. L. Knight, *Phys. Rev. A* **56**, 4175 (1997).
 - [14] M. Ludwig *et al.*, arXiv:1202.0532.
 - [15] K. Stannigel *et al.*, arXiv:1202.3273.
 - [16] J. Dalibard, Y. Castin, and K. Mølmer, *Phys. Rev. Lett.* **68**, 580 (1992).
 - [17] C. W. Gardiner, A. S. Parkins, and P. Zoller, *Phys. Rev. A* **46**, 4363 (1992).
 - [18] H. Carmichael, *An Open Systems Approach to Quantum Optics* (Springer, Berlin, 1993).
 - [19] M. B. Plenio and P. L. Knight, *Rev. Mod. Phys.* **70**, 101 (1998).
 - [20] H. M. Wiseman and G. J. Milburn, *Phys. Rev. A* **47**, 1652 (1993).
 - [21] A. A. Gangat, T. M. Stace, and G. J. Milburn, *New J. Phys.* **13**, 043024 (2011).
 - [22] M. Ueda, N. Imoto, and T. Ogawa, *Phys. Rev. A* **41**, 3891 (1990).
 - [23] L. Mandel and E. Wolf, *Optical coherence and quantum optics* (Cambridge University Press, 1995).
 - [24] V. Parigi *et al.*, *Science* **317**, 1890 (2007).

* Electronic address: andreas.kronwald@physik.uni-erlangen.de